

First-Principles Studies of the Metallization and the Equation of State of Solid Helium

S. A. Khairallah¹ and B. Militzer^{1,2}

¹*Departments of Earth and Planetary Science, University of California, Berkeley, California 94720, USA*

²*Astronomy, University of California, Berkeley, California 94720, USA*

(Received 27 May 2008; published 5 September 2008)

The insulator-to-metal transition in hcp solid helium at high pressure is studied with first-principles simulations. Diffusion quantum Monte Carlo (DMC) calculations predict that the band gap closes at a density of 21.3 g/cm³ and a pressure of 25.7 terapascals, which is 20% higher in density and 40% higher in pressure than predicted by density functional calculations based on the generalized gradient approximation (GGA). The metallization density derived from *GW* calculations is found to be in very close agreement with DMC predictions. The zero point motion of the nuclei had no effect on the metallization density within the accuracy of the calculation. Finally, fit functions for the equation of state are presented, and the magnitude of the electronic correlation effects left out of the GGA approximation are discussed.

DOI: [10.1103/PhysRevLett.101.106407](https://doi.org/10.1103/PhysRevLett.101.106407)

PACS numbers: 71.15.Mb, 02.70.-c, 62.50.-p, 64.30.-t

At low pressure, helium is an inert gas that exhibits a very large electronic excitation gap of 19.8 eV and has the highest ionization energy of all atoms, 24.6 eV. This is because helium has no core electrons, so its valence electrons are bound more strongly than in heavier atoms where screening effects play a role. Given such a strong binding, extreme pressures are needed to reach metallization. After neon [1,2], solid helium is predicted to have the highest metallization pressure among all elemental solids.

Metallic solid helium is expected to be present in the outer layers of white dwarfs (WD) [3]. After the initial star has exhausted all its nuclear fuel, it sheds its outer layer and leaves behind a dense carbon-oxygen core of the size of Earth that is surrounded by an envelope of pure helium, hydrogen, or a mixture. The fossil star then spends the remaining of its lifetime cooling until vanishing luminosity. Measuring the luminosity of the oldest WD would therefore constrain the age of the galaxy [4], which qualifies WDs as stellar chronometers.

Extracting the correct physics from WDs depends on how consistent the cooling models are with the observed luminosity [5]. Characterizing helium at high pressure is important because its properties regulate the heat transport across the outer layers. The metallization transition is important because it marks the point where the heat transfer switches from electronic conduction in interior WD layers to photon diffusion in the exterior.

Most WD models rely on semianalytical descriptions in the chemical picture [3] where one treats helium as a collection of stable atoms, ions, and free electrons interacting via approximate pair potentials. While such approaches work well at low density, they cannot describe the complex interactions in a very dense system; hence, a more fundamental description is required instead. First-principle methods, such as density functional theory and diffusion Monte Carlo (DMC) calculations, are necessary

as they provide a full accounting of quantum and statistical laws that govern the electrons and nuclei.

Properties of fluid helium up to 2 g/cm³ have been the subject of recent calculations. Kietzmann *et al.* [6] relied on DFT and the generalized gradient approximation (GGA) [7] to calculate the electrical conductivity. Kowalski *et al.* [8] used hybrid methods to study the electrical and optical properties and the EOS of fluid helium. Stixrude and Jeanloz [9] studied the band gap closure in fluid helium over a wide range of densities including conditions of giant planet interiors.

In this Letter, we study the pressure metallization in solid helium at densities above 2 g/cm³ using several first-principle simulation techniques. Our intention is to give an assessment of the accuracy of the widely used GGA for calculating band gaps at extreme conditions by considering the *GW* approximation corrections and the accurate, but expensive diffusion quantum Monte Carlo (DMC) method. We study the effect of the zero point motion of the nuclei on the band gap closure and finally derive the equation of state (EOS). We expect our first-principle study to serve as a guide for future laser experiments that are planned to extend the EOS measurements to very high pressures [10].

Our DFT calculations were performed with the ABINIT plane-wave basis code [11]. The electron-nuclei interactions were treated by a local Troullier-Martin norm-conserving pseudopotential [12] with a core radius of 0.4 a.u. We use Perdew-Burke-Ernzerhof GGA [7] for the exchange-correlation functional. We worked with an 8 × 8 × 8 Monkhorst-Pack *k*-point grid and a plane wave energy cutoff of 230 Ha.

Mao *et al.* [13] have demonstrated experimentally that solid helium still remains in the hcp solid phase up to high pressures (57 GPa), apart from a limited fcc loop along the melting line at low temperatures. As a consequence, we

adopt the hcp solid structure and optimize the cell geometry iteratively until the pressure has converged to within 1%.

The band structure in the inset in Fig. 1 shows that solid helium in the hcp structure exhibits an indirect band gap. The lowest unoccupied state occurs at the Γ wave vector. The highest occupied state is at $\mathbf{k} = 0.95\mathbf{k}_M$, which is very close to the M wave vector. Subsequently, we approximate the excitation gap by the difference in energy between the valence M point and the conduction Γ point. As Fig. 1 shows, the band gap decreases almost linearly with increasing density. GGA predicts the band gap closure at a density of 17.4 g/cm^3 , which corresponds to a pressure of 17.0 TPa .

Kohn-Sham GGA is known to systematically underestimate the band gap. DMC calculation is expected to predict the band gap width more accurately because it explicitly includes electronic correlation effects. In fact, DMC has been used successfully to describe the electronic ground state in weakly as well as in strongly correlated systems [14]. Excited states were also calculated reliably with DMC [2,15].

Our DMC simulations were performed with the CASINO code [16]. The trial wave function is of the Slater-Jastrow form and the antisymmetry is maintained by the fixed-node approximation. The electron-electron, electron-nucleus, and electron-electron-nucleus terms in the Jastrow factor were optimized by variance minimization. We use GGA orbitals for the Slater part and keep the same pseudo-

potential as in DFT calculations. A conservative high energy cutoff of 800 Ha is picked. For efficiency, the orbitals are represented using blip functions [17]. The results are well converged with a time step of 0.002 a.u. To calculate the band gap, one electron, in either spin-up or -down, is promoted from the valence band to the conduction band ($M \rightarrow \Gamma$). The calculations for the excited state used the same Jastrow parameters as for the ground state calculation because the DMC energy depends only on the nodes of the trial wave function that are determined by the Slater determinant.

Figure 1 shows the DMC band gaps to be larger than the GGA results, as expected. The DMC curves for the $2 \times 1 \times 1$ and $4 \times 2 \times 2$ rectangular supercells lie parallel to the GGA curve, hence showing a gap correction that is independent of density. DMC simulations in a $4 \times 2 \times 2$ rectangular cell predict a metallization density of $21.3(1) \text{ g/cm}^3$. The $4 \times 2 \times 2$ gap results are converged with respect to system size because the ground state energy agrees to better than 0.1 eV/el with triangular $3 \times 3 \times 3$ supercells. The remaining finite size corrections are small and mostly cancel out upon taking energy differences.

The $4 \times 2 \times 2$ DMC band gaps agree very well with the GW results, which also show a linear behavior with density similar to the GGA and DMC calculations. The GW approximation has proven to be a reliable method for correcting the GGA band gaps in a variety of materials [18]. Our GW band gap corrections are calculated within an accuracy of 0.1 eV after converging the number of bands (50) and plane waves (27 Ha). In comparison, the metallization density is significantly higher than the DFT linear-muffin-tin-orbitals prediction of 13.5 g/cm^3 for helium in the fcc phase [19].

The trial wave function in DMC can be further improved by adding a backflow correction to the Slater determinant. This method introduces further correlation to the trial wave function by replacing the electron coordinates in the determinant by a set of collective coordinates. The DMC total energy decreased slightly, but the band gap did not change within error bars (0.02 eV).

Helium has a long thermal de Broglie wavelength due to its low mass. According to [8,9], the disorder introduced by the zero point motion of the nuclei could reduce the metallization density. We study this effect by calculating the band gap of configurations generated with path integral Monte Carlo (PIMC) [20] simulations at different temperatures between 500 and 5000 K . The helium interaction pair potential was constructed by matching the forces [21] of a density functional molecular dynamics (DFT-MD) simulation at 5000 K . The accuracy of the potential was verified by comparing the original DFT-MD pair correlation function with that of classical Monte Carlo simulations. The computed GGA band gaps for the PIMC configurations were in agreement with the perfect hcp lattice results, within error bars. Hence, the zero point motion had no effect on the band gap.

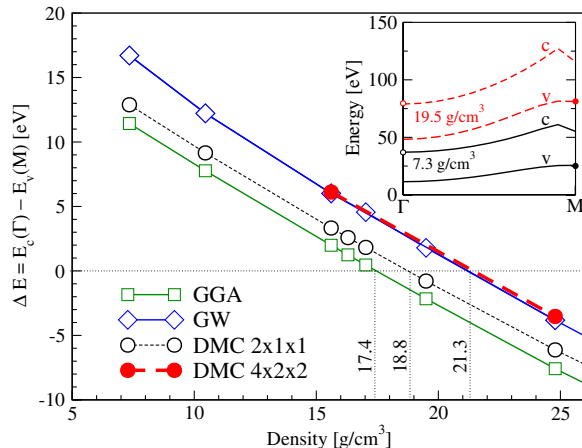


FIG. 1 (color online). Comparison of band gaps as a function of density. DMC results for a small $2 \times 1 \times 1$ rectangular supercell lie parallel and above the GGA gaps by 1.4 eV . DMC ($4 \times 2 \times 2$ rectangular cell) and GW metallization density of $21.3(1) \text{ g/cm}^3$ are in agreement. GGA underestimates the band gap by about 4 eV . The inset shows a part of the electronic band structure including the indirect gap. The filled and open circles indicate, respectively, the highest occupied valence state at the M point and the lowest unoccupied conduction state at the Γ . Two densities are shown. The insulating state (black curve) lies below the metallic state (red dashed curve). The DMC error bars are smaller than the DMC symbols.

DMC is computationally intensive since it scales as high as $O(aN^3 + bN^2)$, where N is the number of electrons. This limits the size of the supercell used to describe well all the correlation effects of the infinite solid and therefore introduces finite size errors. To first order, the independent-particle finite size effects (IPFSE) dominate [22]. The error arises from an incomplete \mathbf{k} -point sampling of the Brillouin zone in the DMC supercell. In DFT, the computational cost is directly proportional to the number of \mathbf{k} -points because the electrons are treated as independent particles. In DMC, however, more \mathbf{k} -points are included in bigger cells, as long as they obey periodic boundary conditions. To include the Γ and M wave vectors into one DMC band gap calculation, we have chosen rectangular $2 \times 1 \times 1$ (16 electrons and 2 \mathbf{k} -points) and $4 \times 2 \times 2$ (128 electrons and 12 \mathbf{k} -points) primitive unit cells. This choice is prescribed by the boundary condition $(k_i \mathbf{b}_i) \cdot (l_j \mathbf{a}_j) = 2\pi \delta_{ij} m$, where m is an integer, $k_i \mathbf{b}_i$, $l_j \mathbf{a}_j$ are, respectively, the components of the wave vector and the supercell length along the reciprocal and Bravais primitive vectors. We calculate the IPFSE from the formula, $E_\infty = E_N^{\text{DMC}} + (E_\infty - E_N)^{\text{GGA}}$, where $(E_\infty - E_N)^{\text{GGA}}$ can be calculated cheaply with GGA, and corresponds to the difference between a converged GGA with respect to \mathbf{k} -point sampling and a GGA result for the same DMC cell size. By comparing energies of different cell sizes, we determined the energy to be converged for $3 \times 3 \times 3$ triangular (108 electrons) cell sizes and bigger. The IPFSEs range from 0.07 eV/el up to 2.0 eV/el with increasing density. Kinetic energy corrections of the order of 0.1 eV/el due to long range correlations [23] are also included.

The Coulomb finite size effects (CFSE) are also considered. They emerge from treating the electronic correlations periodically whereby the exchange-correlation (XC) energy would include periodic XC hole contributions. These effects decay with system size as $1/N$ and tend to lower the energy slightly. We avoid these effects by using the model interaction potential (MPC) instead of the Ewald interaction [14]. The difference between the total ground state energies computed with these two interactions is 0.04 eV/el for the highest density. The error increases with density because the periodic image charges are closer in smaller volumes. We obtain very similar band gaps with the Ewald and the MPC interactions. This is due to the cancellation of CFSE errors when taking energy differences to calculate the gap.

After correcting the DMC ground state energies for finite size effects, we compare with converged GGA energies, E_{DFT} , calculations in Fig. 2. We estimate the correlation energy that is missing in GGA in two ways. First, we report the difference $E_{\text{DMC}} - E_{\text{DFT}}$ for the $3 \times 3 \times 3$ supercell. Second, we extrapolate the DMC energies in $E_{\text{DMC}} - E_{\text{DFT}}$ to infinite size as a function of $1/N$ using a linear and a quadratic fit. This step involves DMC calculations over different cell sizes. The resulting error bars in Fig. 2(a) are small except for the highest density, i.e.,

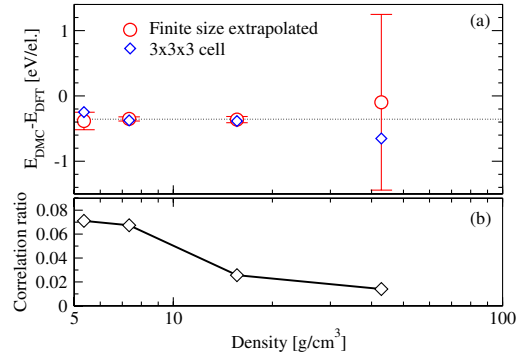


FIG. 2 (color online). Panel (a): Difference between DMC and GGA ground state energies. We calculate the DMC energy in two ways, by extrapolations to infinite cell size (circles) and by directly using results from our largest $3 \times 3 \times 3$ triangular supercell (diamonds). In panel (b), we relate the DFT-DMC energy difference to the amount of mechanical work needed to reach a certain density. We plot the correlation fraction, $(E_{\text{DFT}} - E_{\text{DMC}})/(E_{\text{DFT}} - E_{\text{atom}})$, where $E_{\text{atom}} = -79.0048$ eV is the exact energy of the isolated helium atom.

smallest volume. In the density range of consideration, the correlation energy error in GGA is approximately constant, 0.36 eV/el.

The correlation error in GGA becomes less important with increasing density because it stays constant while the energy increases with compression. The relative importance of the correction energy is illustrated in Fig. 2(b), where we compare the energy difference $E_{\text{DMC}}(\rho) - E_{\text{DFT}}(\rho)$ to the energy needed to compress helium to density ρ , $E_{\text{DFT}}(\rho) - E_{\text{atom}}(\rho = 0)$. This choice for comparison does not depend on the zero of energy. Since DMC yields the exact result for the helium atom, the correlation ratio, $[E_{\text{DFT}}(\rho) - E_{\text{DMC}}(\rho)]/[E_{\text{DFT}}(\rho) - E_{\text{atom}}(\rho = 0)]$, approaches unity in the infinitely low density limit. In the opposite high density limit, the graph shows how it tends to zero as helium approaches the state of a one-component plasma with a neutralizing background. The kinetic energy of the homogeneous electron gas dominates the correlation and eventually the Coulombic energy terms. GGA is expected to describe this limit well since the exchange-correlation functional was derived from DMC simulations of the homogeneous electron gas [24].

Since the corrections to the GGA energy appear to be independent of density, there are no corrections to pressures derived from GGA. We were able to represent our zero-temperature static lattice GGA pressure data in the insulating regime by a Vinet EOS curve [25] with the parameters $V_0 = 20.6397$ cm³/mol as zero-pressure volume, $B_0 = 0.01928$ GPa as bulk modulus, and $B'_0 = 9.2153$ as its derivative. The fit reproduced our GGA data from 3 to 1200 GPa with an accuracy of 3%. The comparison with experiments [26] was studied in great detail earlier [27].

It was not possible to extend the Vinet fit into the metallic regime. Instead, we adopt a fit based on the

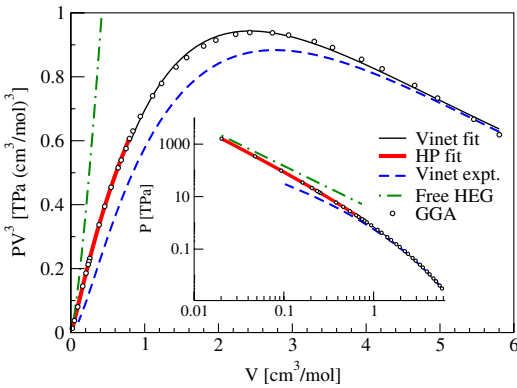


FIG. 3 (color online). Pressure-volume relationship derived from GGA calculations for solid helium. The experimental Vinet fit [26], valid up to 57 GPa, agrees with the low pressure Vinet fit of GGA data. The high pressure (HP) fit to the GGA data approaches the free homogeneous electron gas (HEG). To emphasize differences, PV^3 was plotted in the main graph.

parametrization of the homogeneous electron gas energy. This fit includes the kinetic, Coulombic, exchange as well as correlation terms and, in this case, also ionic contributions, $P(V) = \frac{a_1}{V^{5/3}} + \frac{a_2}{V^{4/3}} + \frac{a_3}{V} + \frac{a_4}{V^{2/3}}$. In units of GPa and cm^3/mol , the coefficients are $a_1 = 3186.21$, $a_2 = -2761.74$, $a_3 = -565.78$, and $a_4 = 854.71$ where the leading coefficient is taken from the free Fermi gas. The fit reproduces our DFT data points from 1.2 to 1600 TPa within 0.5%. In Fig. 3, we show the pressure over a large density range. In the high density limit, the correlation effects decrease, and the DFT pressure approaches the free homogeneous electron gas behavior.

In conclusion, we have demonstrated that solid helium reaches a metallic state at an extreme pressure of 25.7 TPa, which is significantly larger than predicted by standard GGA method. For WD interiors, this implies that the inner layer of metallic helium is thinner and the outer region where photon diffusion dominates the heat transport is larger than previously predicted.

With quantum Monte Carlo, we have shown that standard GGA methods underestimate the band gap in solid helium by 4 eV, which translates into an underestimation of the metallization pressure by 40%. The *GW* band gap corrections are in good agreement with DMC calculations, which offers the possibility of using *GW* for correcting the band gaps derived from GGA simulation of fluid helium at high pressure and to make more realistic comparisons with shock wave measurements of conductivity and reflectivity.

Finally, we determined the equation of state and presented a fit. We analyzed the correlation effects that are missing in GGA and demonstrated that their importance decreases relative to the total energy with increasing den-

sity as helium approaches the state of a one-component plasma with a rigid neutralizing background.

This work was supported by NSF and NASA. We thank the Cambridge group for the CASINO code. NERSC provided computational resources. We acknowledge useful discussions with E. Quataert, P. Chang, and R. Jeanloz.

-
- [1] J. C. Boettger, Phys. Rev. B **33**, 6788 (1986).
 - [2] N.D. Drummond and R.J. Needs, Phys. Rev. B **73**, 024107 (2006).
 - [3] C. Winisdoerffer and G. Chabrier, Phys. Rev. E **71**, 026402 (2005); V.E. Fortov *et al.*, JETP **97**, 259 (2003).
 - [4] T.D. Oswald, J.A. Smith, M.A. Wood, and P. Hintzen, Nature (London) **382**, 692 (1996).
 - [5] J. Isern, E. García-Berro, M. Hernanz, and G. Chabrier, Astrophys. J. **528**, 397 (2000); Brad M.S. Hansen, Astrophys. J. **520**, 680 (1999); S.K. Leggett, M.T. Ruis, and P. Bergeron, Astrophys. J. **497**, 294 (1998).
 - [6] A. Kietzmann *et al.*, Phys. Rev. Lett. **98**, 190602 (2007).
 - [7] J.P. Perdew, K. Burke, and M. Ernzerhof, Phys. Rev. Lett. **77**, 3865 (1996).
 - [8] P.M. Kowalski *et al.*, Phys. Rev. B **76**, 075112 (2007).
 - [9] L. Stixrude and R. Jeanloz, Proc. Natl. Acad. Sci. U.S.A. (to be published).
 - [10] W.J. Nellis *et al.*, Phys. Rev. Lett. **53**, 1248 (1984); J. Eggert *et al.*, Phys. Rev. Lett. **100**, 124503 (2008).
 - [11] X. Gonze *et al.*, Z. Kristallogr. **220**, 558 (2005).
 - [12] M. Fuchs and M. Scheffler, Comput. Phys. Commun. **119**, 67 (1999).
 - [13] P. Loubeyre *et al.*, Phys. Rev. Lett. **71**, 2272 (1993).
 - [14] W.M.C. Foulkes, L. Mitás, R.J. Needs, and G. Rajagopal, Rev. Mod. Phys. **73**, 33 (2001).
 - [15] L. Mitás and R.M. Martin, Phys. Rev. Lett. **72**, 2438 (1994).
 - [16] R.J. Needs, M.D. Towler, N.D. Drummond, and P. Lopez Rios, CASINO 2.1 (Univ. of Cambridge, Cambridge, England, 2005).
 - [17] D. Alfè and M.J. Gillan, Phys. Rev. B **70**, 161101 (2004).
 - [18] K.A. Johnson and N.W. Ashcroft, Phys. Rev. B **58**, 15548 (1998).
 - [19] D.A. Young, A.K. McMahan, and M. Ross, Phys. Rev. B **24**, 5119 (1981).
 - [20] D.M. Ceperley, Rev. Mod. Phys. **67**, 279 (1995).
 - [21] S. Izvekov *et al.*, J. Chem. Phys. **120**, 10896 (2004).
 - [22] P.R.C. Kent *et al.*, Phys. Rev. B **59**, 1917 (1999).
 - [23] S. Chiesa, D.M. Ceperley, R.M. Martin, and M. Holzmann, Phys. Rev. Lett. **97**, 076404 (2006).
 - [24] D.M. Ceperley and B.J. Alder, Phys. Rev. Lett. **45**, 566 (1980).
 - [25] P. Vinet *et al.*, Phys. Rev. B **35**, 1945 (1987).
 - [26] P. Loubeyre *et al.*, Phys. Rev. Lett. **71**, 2272 (1993).
 - [27] C.P. Herrero, J. Phys. Condens. Matter **18**, 3469 (2006); C. Cazorla and J. Boronat, *ibid.* **20**, 015223 (2008).